DESCRIPTORS FOR SEA SURFACE TEMPERATURE FRONT REGULARITY CHARACTERIZATION

Silèye O. Ba[*]*, Ronan Fablet*[*]*, Dominique Pastor*[*]*, Bertrand Chapron*[♮]*,*

Lab-STICC[*], Université Européenne de Bretagne, Technopole Brest Iroise, Plouzané, 29238, France
CERSAT [♮], IFREMER, Technopole Brest Iroise, Plouzané, 29238, France

1. INTRODUCTION

Monitoring sea surface temperature (SST) is of high interest. The dynamics of climatic events such as tropical storms or cyclones are closely related to the sea surface temperature [1, 2]. An important research topic in oceanography is about the understanding of the interactions between the ocean's surface and it's deeper layers [3–5]. In [3] Lapeyre et al show that in the case of baroclinic unstable flows, the potential vorticity of mesoscale and submesoscale structures in the ocean interior are strongly correlated to the surface density structures. Thus, in frontal regions, knowledge of the ocean surface structures regularity would give insights about the 3D dynamics of the ocean. In this paper we address this issue and focus on the analysis of the SST images level lines regularity from satellites images in regions in the neighborhood of oceanic fronts. Two regions of interest are considered: the region of Benguela and the region of Malvinas. Our investigations suggest that SST fronts belong to the class of statistical self similar curves. Taking into account self similar curves properties, we propose local curvature based descriptors for SST front region regularity characterization. We experimentally assess the efficiency of our descriptors by measuring their ability to capture seasonal variations. The remaining of this paper is organized as follows. Section 2 gives arguments allowing to conclude that SST fronts can be considered as statistically self similar curves. Section 3 presents the SST image regularity descriptors we propose. Finally, the experiments we conducted to assess the effectiveness of the descriptors are presented in Section 4.

2. SST FRONTS AS STATISTICAL SELF-SIMILAR CURVE

The characterization of the level-lines of the SST maps, specially in SST fronts regions, is viewed as a mean for characterizing and discriminating ocean turbulence patterns. Level lines, specially SST fronts, are intrinsically high dimensional objects which makes difficult their characterization. Statistical tools exist to characterize specific class of curves such as statistical self similar curves.

Mandelbrot proposed characterizations for a certain class of self similar curves f_t called fractional Brownian motion (FBM) which have self similar increments [6]. These processes verify that, for any $h > 0$, $f_{t+\tau} - f_0$ and $\frac{1}{h^H}(f_{t+h\tau} - f_0)$ have the same joint distribution. Using the self similarity property, for any $h > 0$, the covariances of the process increments verifies $\mathbb{E}(f_{t+h\tau} - f_0)^2 = h^{2H}\mathbb{E}(f_{t+\tau} - f_0)^2$ where H is a regularity parameter usually denominated the Hurst parameter. The Hurst parameter can be obtained using a least square error estimation from the relation

$$2H\log(h) = \log\mathbb{E}(f_{t+h\tau} - f_0)^2 - \log\mathbb{E}(f_{t+\tau} - f_0)^2 \quad (1)$$

given a sample path of the curve f_t. The validity of the assumption that SST fronts are realization of FBM processes can be assessed by verifying to which extent the rule in Eq. 1 is verified. Given an SST level-line, we consider the goodness of fit of the regression line as a valid experimental diagnosis. Fig. 1(a) a gives a sample image of the region of Benguela with the SST detected front marking the separation between northern warm waters and southern cold waters. Fig. 1(b) depicts the regression line corresponding to Eq. 1. These figures show that the ratio of the variance is very well represented by the regression of the time scales. Thus, we can conclude that the fronts can be very well represented as FBM realizations.

An interesting sub-class of self similar curves is the class of conformally invariant curves. The properties of conformally invariant curves have been widely studied in physics as they appear at the criticality of phenomena such as percolation, turbulence, mechanics [7]. Considering SST fronts as the results of critical phenomena occurring in the ocean, we aim at testing the hypothesis that SST fronts are conformally invariant curves. A remarkable property of conformally invariant curves relates to the statistics of their winding angles. The winding angle θ is defined as the angle between the line joining two points separated by a length L along the curve and the local tangent at the reference point. The probability distribution of the winding angles is a centered Gaussian law with a variance $\mathbb{E}\theta^2 = 4\log L$ that logarithmically increases with the distance to the reference point [8]. Boffetta *et al* used this property to show that the rocky shorelines of Brittany are conformally invariant [9]. Fig. 1(c) reports the distribution of the variance of the winding angles as a function of the length along the curve for the front detected in an SST observation of the Agulhas region the 20th of february 2008. Though not being perfect as in the example considered by Boffeta *et al* [9], the fit to the conformally invariant model depicts a satisfactory correlation. It should be stressed that theoretical work addressing turbulence dynamics exploited high-resolution observation. In contrast, the considered SST images are rather low-resolution images (25km gridding). Besides, gridded SST data result from different processing steps including interpolation of

This work was partially funded by the Brittany Council's CREATE program through the FI2O 2009-2011 Project.

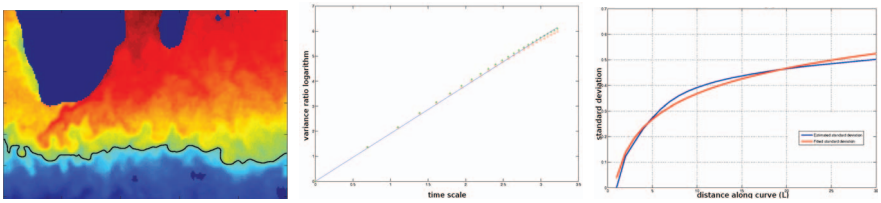

(a) Benguela front (b) Self similarity regression (c) Winding angles distribution.

Fig. 1. SST fronts as FBM or conformally invariant processes realization. Fig.1(a) gives the detected front. Fig 1(b) shows plot logarithm of the time scale versus the logarithm of the scaled variance ratio (dots) and the line fitted to these points using least square regression. Fig.1(c) gives the plot of the winding angles distribution.

missing data. These characteristics of SST observations may impact the statistical properties of SST level-lines. Overall, these results support the hypothesis that SST level-lines at frontogenesis belong to the class of the conformally invariant curves in relation to the nature of the turbulence dynamics undergone by the ocean. Conversely, the regularity of these SST level-lines can be regarded as signatures of the nature of the turbulence.

The analysis conducted in this section suggests that fronts can be considered as self similar curves. Thus curvature based descriptors capturing the local angles variations should be good candidates to characterize the nature of ocean dynamics from SST images.

3. SST IMAGE REGULARITY DESCRIPTORS

3.1. Iso-temperature extraction

The approach we propose to characterize the geometric regularity of a front region in an SST image is based on the local curvature statistics along iso-temperatures. The computation of curvature statistics can be performed at various image scale. Thus, an anisotropic diffusion pre-processing step with different scale parameters is applied to the images. More precisely we apply a diffusion by mean curvature motion (MCM) that guarantees the conservation of the topology of the hierarchical image level set representation [10]. The extraction of iso-temperature curves in SST images is based on the fast level-set transform (FLST) proposed in [11]. This method allows to extract a hierarchical representation of a scalar image invariant to contrast changes.

3.2. SST Image Regularity Descriptors

For each level line, we consider as regularity descriptor the marginal distribution of its local curvatures. We followed three approaches to extract the local curvatures of the level lines.

Local tangents derivatives: To compute the curvature of the level lines we can compute the variations of the directions of the level line local tangents. If we denote by $f(s) = (x(s), y(s))$ the level line parameterized by its curvilinear abscissa s, the orientation of the local tangent is given by $\theta(s) = \left|\arctan\left(\frac{\dot{y}(s)}{\dot{x}(s)}\right)\right|$ where $\dot{x}(s)$ is the derivative of x with respect to s. An estimate of the local curvature can be obtained by the difference between the direction of the local tangents $\kappa(s) = |\theta(s) - \theta(s-1)|$.

Direct curvature computation: Rather than computing the derivatives of the local tangents orientation, the curvature of the level line $f(s) = (x(s), y(s))$ can be directly computed according to the formula $\kappa(s) = \frac{\ddot{x}(s)\dot{y}(s) - \dot{x}(s)\ddot{y}(s)}{|\dot{x}(s) - \dot{y}(s)|^{\frac{3}{2}}}$ where $\ddot{x}(s)$ is the second derivative of $x(s)$ w.r.t. the curvilinear abscissa s.

SST image divergence: The curvature of the level lines can also be derived a classical partial difference operator to the SST image pixels. This operator is given as the divergence of the normalized image gradient defined as:

$$\text{curv(u)} = \text{div}\left(\frac{\nabla u}{|\nabla u|}\right) = \frac{u_{xx}u_y^2 - 2u_{xy}u_x u_y + u_{yy}u_x^2}{|\nabla u|^3} \tag{2}$$

3.3. Image classification based on the regularity descriptors

We aim at evaluating the relevance of curvature statistics for the discrimination of ocean turbulence patterns at frontogenesis. Assuming that seasons refer to different turbulence regimes, we consider a classification issue where the classes are the seasons and the features associated with each SST image are curvature statistics. For a given class, the geometric regularity of the class is given by the global distribution over the training samples of the class. The classification of a new SST observation at frontogenesis is achieved using a nearest neighbors criterion, according to the Battacharya distance, between the descriptors of the image and the descriptors of the seasons. The Battacharya distance between two histograms $p = (p_k, k = 1, .., K)$ et $q = (q_k, k = 1, .., K)$ is defined as $\rho(p, q) = \sqrt{1 - \sum_{k=1}^{K} \sqrt{p_k}\sqrt{q_k}}$. We used the Battacharya distance because it is well suited to compare histograms. Other histogram specific distances such as the Kullback-Liebler divergence could have been used.

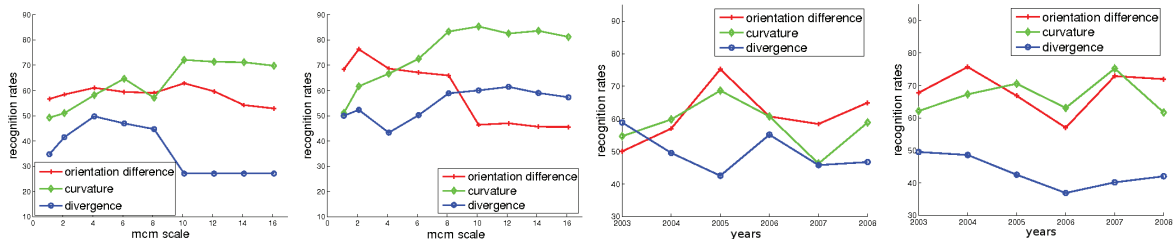

(a) Benguela (b) Malvinas (c) Benguela (d) Malvinas

Fig. 2. Classification performances. Fig. 2(a) and 2(b) give the average classification performances over the 6 years season classification for Benguela and Malvinas for varying smoothing scales. Fig. 2(c) and 2(d) give the yearly classification performances for Benguela and Malvinas.

4. EXPERIMENTS

4.1. Evaluation Protocol

A quantitative evaluation is carried out from the Remote Sensing System (RemSS) SST TMI-AMRE-OI images database [12] [1]. The database consists in daily global SST images recorded since the first of June 2002 to nowadays. For our evaluation we used data from the years 2003 to 2008, with a 20 day buffer between seasons for two regions depicting particular ocean dynamics: the Aghulas current and the Malvinas region. Let us point out that the seasons are denominated according to the south hemisphere terminology: summer corresponds to the period between December to march. We selected these regions because they involve important oceanic fronts. The region Benguela region is localized between $[-30°, -50°]$ of latitudes and $[10°, 70°]$ of longitudes. The Malvinas area is localized between $[-30°, -60°]$ of latitudes and $[290°, 330°]$ of longitudes.
To evaluate our descriptors, first we assess their seasonal discrimination potential by verifying that for a given descriptor, the intra-season distance and the inter-season distance are significantly different. Then, considering a season based classification task, in turn the data of one year is used as test data, while the data of the remaining years are used to learn seasons descriptors.

4.2. Statistical variabilities of the Descriptors

To evaluate the statistical significance of the difference between the intra-class and the inter-class distance we used the following non parametric approach. [2]. Given two classes, $\mathcal{S}_1$ and $\mathcal{S}_2$, and the descriptors extracted from the SST images that belong these classes, $p_{1,i}$ and $p_{2,j}$, that we want to test the difference. We use the following criterion, inspired from the Fisher statistics,

$$F = \frac{\rho(\mu_1, \mu_2)}{\sqrt{\frac{1}{|\mathcal{S}_1|}\sum_i \rho(p_{1,i}, \mu_1) + \frac{1}{|\mathcal{S}_2|}\sum_{j \in C_2} \rho(p_{2,j}, \mu_2)}} \tag{3}$$

where μ_1 et μ_2 are the classes descriptors. The principle of the non-parametric test built on the measure in Eq. 3 is the following. First we group the descriptors of the two classes in a unique set. Then, we generate a given number of Fisher statistics by generating two bootstrapped classes uniformly sampled from from the unique set. Those bootstrapped fisher samples allows to build a non parametric density distribution $p(F)$ of the Fisher statistic on the grouped class. Then we calculate the Fisher statistics of the two original classes $F_{1,2}$. The decision of the difference between the descriptors in the two classes is taken according to the value of $p(F > F_{1,2})$. If $p(F > F_{1,2})$ is very small, the descriptors are considered to be different.

We applied this test to the task of discriminating the season using the descriptors described in Section 3.2 and applied to the two datasets: the Aghulas region and the Malvinas area. In all cases, we obtained $p(F > F_{1,2}) < 0.001$. It can be concluded that the regularity of SST images depicts significant seasonal differences. This conclusion is in adequacy with [13] which showed that ocean SST exhibit seasonal vorticities, i.e. seasonal variations of the turbulence patterns.

4.3. Regularity-based Classification

Fig. 2(a) and 2(b) give the average performance over the task of classifying days into seasons given varying smoothing scales using the three types of features described in Section 3.2. These figures show that the performance with the difference of the level lines local tangent orientation, and for the level lines curvatures are better than with the image divergence. The lower recognition rate obtained with the image divergence could be explained by the numerical instability of the computation of the divergence operator. Also, better classification performance are reported for the region of Malvinas compared to the region of Benguela. Sharper vorticity structures in the Malvinas could explain these performance. The yearly performance presented in Fig. 2(c) and 2(d) show that the conclusions drawn about the performance of

[1] The RemSS database is publicly available at `http://remss.com/sst/`. More information about the technical aspects can be found in [12].
[2] The main motivation for using a non-parametric test is that it doesn't require any assumption on the data underlying distribution.

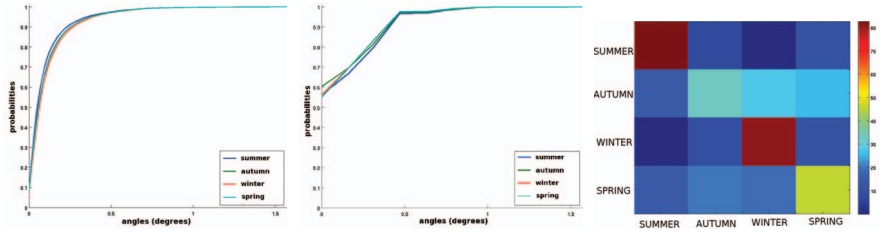

(a) Local tangent orientation difference.

(b) Image divergence.

(c) Local tangent orientation difference.

Fig. 3. Model cumulative distributions (Fig. 3(a) and 3(b)), and classification confusion matrix (Fig. 3(c)).

the various features hold at a yearly level. The tangent direction differences and the curvatures lead to better performance than the divergence. Furthermore, the classification performance for the region using data from the region of Malvinas are higher than the one obtained using data from the region of Benguela. However, a detailed analysis of the performance over the years shows variabilities across the years.

The performance of the descriptors we proposed can be evaluated at a finer level by analyzing the confusion matrices obtained using each one of the descriptors. Fig.3(c) gives the confusion matrix the iso-temperatures local tangent direction difference for the region of Benguela. This figure shows that summer and winter are well recognized with recognition rates greater than 70%. While there is more confusion for the recognition of autumn and spring. These confusions can be explained by the transitory nature of these seasons. The regularity of the iso-temperatures are less typical than for summer and winter. When analyzing the confusion matrices we can notice that there no privileged types of confusions. Autumn and spring are confused with all the other seasons. Fig. 3(a) and 3(b) give the cumulative distributions modeling the SST images regularity for each season. We can notice that winter is the season for which the SST are the less regular because its marginal distribution exhibits the slowest decay. While summer is the most regular season. These results show that the proposed descriptors are able to capture seasonal SST regularities. Because SST regularity at frontogenesis is related to oceanic vorticities resulting from turbulence, the proposed descriptors could be seen as valid signatures of tuburbulent activities.

5. REFERENCES

[1] H. Giordani and G. Caniaux, "Sensitivity of cyclogenesis to sea surface temperature in the northwestern atlantic," *Monthly Weather Review*, pp. 1273–295, 2001.

[2] M. A. Saunders and A. S. Lea, "Large contribution of sea surface warming to recent increase in atlantic hurricane activity," *Nature*, pp. 557–560, 2008.

[3] G. Lapeyre and P. Klein, "Dynamics of the upper oceanic layers in terms of surface quasigeostrophy theory," *Journal of Physical Oceanography*, pp. 165–176, 2006.

[4] G. Lapeyre, P. Klein, and B. L. Hua, "Oceanic restratification forced by surface frontogenesis," *Journal of Physical Oceanography*, pp. 1577–1590, 2006.

[5] X. Capet, J. McWilliams, M. J. Molemaker, and A. Shchepetkin, "Mesoscale to submesoscale transition in the california current system. part i: Flow structure, eddy flux, and observational tests," *Journal of Physical Oceanography*, 2008.

[6] B. B. Mandelbrot and J. van Ness, "Fractional brownian motions, fractional noises and applications," *SIAM Review*, pp. 422–437, 1968.

[7] M. Henkel, *Conformal Invariance and Critical Phenomena*. Springer, 1999.

[8] B. Duplantier and H. Saleur, "Winding-angle distribution of two dimensional self avoiding walk from conformal invariance," *Physical review letter*, pp. 2343–2346, 1988.

[9] G. Boffetta, A. Celani, D. Dezzani, and A. Seminara, "How winding is the coast of britain? conformal invariance of rocky shorelines," *Geophysical research letters*, 2008.

[10] L. Alvarez, F. Guichard, P.-L. Lions, and J.-M. Morel, "Axioms and fundamental equations of image processing," *Archive for Rational Mechanics and Analysis*, pp. 199–257, 1993.

[11] P. Monasse and F. Guichard, "Fast computation of a contrast-invariant image representation," *IEEE Transactions on Image Processing*, pp. 860–872, 2000.

[12] F. Wentz, P. Ashcroft, and C. Gentemann, "Post-launch calibration of the TMI microwave radiometer," *IEEE Transactions on Geosciences and Remote Sensing*, pp. 415–422, 2001.

[13] Q. Yang, B. Parvin, A. J. Mariano, E. H. Ryan, R. Evans, and B. O. Brown, "Seasonal and interannual studies of vortices in sea surface temperature data," *International Journal of Remote Sensing*, pp. 1371–1376, 2004.